ZIBELINE INTERNATIONAL™ PUBLISHING

ISSN: 2521-0890 (Print)
ISSN: 2521-0491 (Online)
CODEN: GBEEB6

Geological Behavior (GBR)

DOI: http://doi.org/10.26480/gbr.02.2021.59.66

RESEARCH ARTICLE

INTEGRATED GEOPHYSICAL MAPPING OF GROUNDWATER AQUIFER FOR SPATIAL DISTRIBUTION OF GROUNDWATER DEVELOPMENT IN IPERINDO AND ITS ENVIRONS, SOUTHWESTERN NIGERIA

Kazeem O.Olomo [a *], Oluwatoyin K. Olaleye [b], Temitayo O. Ale[a], Michael T. Asubiojo [a], Oluyemi E. Faseki[b]

[a] Department of Earth Sciences, Adekunle Ajasin University, Akungba-Akoko, Nigeria
[b] Department of Applied Geophysics, Federal University of Technology, Akure, Nigeria
****Corresponding author email: kazeeem.olomo@aaua.edu.ng***

This is an open access article distributed under the Creative Commons Attribution License, which permits unrestricted use, distribution, and reproduction in any medium, provided the original work is properly cited.

ARTICLE DETAILS

Article History:

Received 06 October 2021
Accepted 08 November 2021
Available online 23 November 2021

ABSTRACT

Assessment of groundwater potential of Iperindo area, Southwestern Nigeria was conducted by mapping spatial distribution of groundwater availability within the area and consequently locating areas of groundwater reserve to serve the community and its environs. This was achieved by integrating geophysical techniques involving landsat ETM-7 satellite data, aeromagnetic data, VLF-EM and electrical resistivity methods to delineate subsurface structures, understand the direction of groundwater flow, and detect the depth to groundwater aquifer. The result of landsat and aeromagnetic revealed some lineament intersection approximately NE-SW direction and interpreted to be potential sites for groundwater development. VLF-EM revealed geologic structures of significant hydrogeological importance at depths of 40 m to 200 m. Vertical electrical sounding (VES) confirmed high groundwater prospect in the areas with estimated depth to water table between 30 m and 100 m. The integrated results of the study revealed adequate groundwater spatial distribution for effective groundwater development in the area.

KEYWORDS

aeromagnetic, aquifer, geologic structure, hydrogeology, landsat.

1. INTRODUCTION

Water is a basic need critical to human life because it contains nutrients that help human body functionality. Its importance includes the support for food digestion, absorption, nutrients use and transportation, and elimination of toxins and wastes from the body. Adequate provision of safe domestic water is a health protecting measure. The quality and quantity of water people use depends on the ease to access it. Improving the access to safe water supply is a major health challenge for the World Health Organisation (WHO) and United Nations Children's Fund (UNICEF). Availability of potable water is one of the major challenges in Nigeria and other developing countries. Statistics show that access to improved water was 39 % in 1999, while access to safe water was 50% in 1995 and 54% in 1999 in Nigeria (Federal Government of Nigeria and United Nations Children's Fund, 2001).

Rapid mining activities by the illegal miners currently witnessed at study area have resulted into poor access to potable water. Protected dug wells and borehole water pumps are not readily available in this area. People largely depend solely on water from streams and hand-dug wells for both commercial and domestic uses. Apart from untold hardship that people are facing owing to inadequate quality water, the available sources of water are vulnerable to pollution as result of runoff water from the processed mined gold. This has made the people to be prone to water-borne related diseases such as diarrhea, intestinal worms, cholera, dysentery and typhoid fever. One of the scientific recommended approaches to improve access to potable water is to carry out geological and geophysical investigation to locate groundwater site that is free from contamination before placing a borehole (Olomo, 2021). Groundwater is generally controlled by weathered and fractured basement rocks especially in the basement area (Wright, 1992; Olorunfemi and Fasuyi, 1993). The basement aquifers are often discontinuous laterally and vertically due to the presence of fault (Satpathy and Kanugo, 1976). These natures of the basement aquifer system make the adoption of geophysical investigations method possible to unravel the subsurface geology, weathered depth and structural setting.

Several Geophysical methods such as electrical resistivity, gravity, magnetic, seismic and electromagnetic have proven to be reliable through which hydrogeological significant features can be mapped (Eaton and Watkins, 1970; Vanderberghe, 1982). Integration of aeromagnetic and remote sensing methods data recently becomes highly effective tool for investigating groundwater resource exploration (Batista-Rodriguez et al., 2017; Hung et al., 2005). Aeromagnetic method has been found to be very successful in delineating various subsurface formations due to relatively high susceptibility contrast between basement rocks (Emujakporue et al., 2017; Osinowo et al., 2013; Steinich et al., 1999; Srivastava, 2002). Electrical resistivity method provides a significant resistivity contrast between deposit overburden and the underlying bedrock (Ako and Olorunfemi, 1989). Very Low Frequency Electromagnetic (VLF–EM) method is useful in groundwater investigation in basement terrain, to appreciably map thick overburden and geological structures such as fault and fracture zones that are favorable to groundwater accumulation (Amadi and Nurudeen, 1990; Olorunfemi et al., 1995; McNeill, 1980; Palacky et al., 1981).

Quick Response Code	Access this article online	
	Website: www.geologicalbehavior.com	**DOI:** 10.26480/gbr.02.2021.59.66

Cite The Article: Kazeem O.Olomo , Oluwatoyin K. Olaleye , Temitayo O. Ale, Michael T. Asubiojo , Oluyemi E. Faseki (2021). Integrated Geophysical Mapping of Groundwater Aquifer for Spatial Distribution of Groundwater Development in Iperindo and Its Environs, Southwestern Nigeria, *Geological Behaviour 5(2): 59-66.*

In this work, groundwater potential of the study area was assessed by mapping the spatial distribution of groundwater availability within the study area and consequently decides the best location for the groundwater reserve. Reconnaissance exploration works for the hydrogeology study was conducted using airborne method to provide spatial first-hand information about the basement. Ground survey of electromagnetic VLF-EM method and vertical electrical sounding VES were also conducted to confirm the airborne results and delineate groundwater prospect zones. The work is based on the assumption that groundwater in crystalline basement mainly occur in fractured and weathered zone of the basement.

2. Description of The Study Area and Geologic Setting

The study area is Iperindo in Atakunmosa East local Government Area in Osun State Nigeria. Iperindo and its environs are located on the crystalline basement complex and falls within latitude 7° 30' 20.82" N to 7o 33"2.89" N and longitude 4° 48' 44.83" E to 40 51" 28.58" E (Figure 1). It has an area of 238Km2 and a population of 76,197 at the 2006 census. Iperindo area is an upland and resistant to weathering and erosion. The topography is undulating and punctuated in some areas by hilly ridges and gently steeping landforms. There are low lying outcrops in the few exposures in the study area. The study area is over 400m above sea level except few areas that fall just below 400m with some hills at the northern part of the study area. The ridges are formed by quartz-schist and quartzite that rises abruptly from enveloping basins and trend in west to east section. The drainage system is dominated by dendritic pattern of streams flows, which is typical of the basement complex terrain and are structurally controlled. The study area belongs to the Southwestern Nigeria basement complex comprising Migmatite-gneiss complex, Quartz-Shcist, Quartzite and Amphibolites. Other minor rocks are Garnet, Quartz chlorite bodies and Dolorites (Odeyemi, 1993).

3. Materials and Method

The remote sensing data employed in this study is the LANDSAT 7 enhanced thematic mapper plus (ETM+) downloaded from USGS website (www.usgs.com). An aeromagnetic data scale of 1:50,000 were procured from the Nigerian Geology Survey Agency (NGSA). Regional correction was based on IGRF. ABEM Wadi VLF measuring instrument was used in measuring the EM response by measuring the electrical properties of the subsurface through EM induction. It maps the conductive zones of the environment. VLF has a stable transmitter, which is developed and planted all over the world for military purpose in term of war; and a movable receiver which is the equipment used on field. The equipment is made up of three units; the receiving unit, the antenna unit, the power unit, and the horizontal and vertical bars.

The equipment measures the real component, the imaginary quadrature, current density and the filtered real component. Traverses were made perpendicular to the general geologic strike. For the resistivity survey, resistivity meter (SAS 4000) made up of the power source (direct current of 5-500mA) and the potential measuring device/voltmeter (direct current voltmeter ranging between 10mV-20V) was utilized. Preliminary study was carried out by mapping processing the landsat and aeromagnetic survey data of the study area. This is done in order to isolate the areas that have high groundwater potential through the delineation of lineament from both landsat and aeromagnetic investigation. Thereafter, detailed investigation was carried out to confirm the result of preliminary investigation from airborne survey.

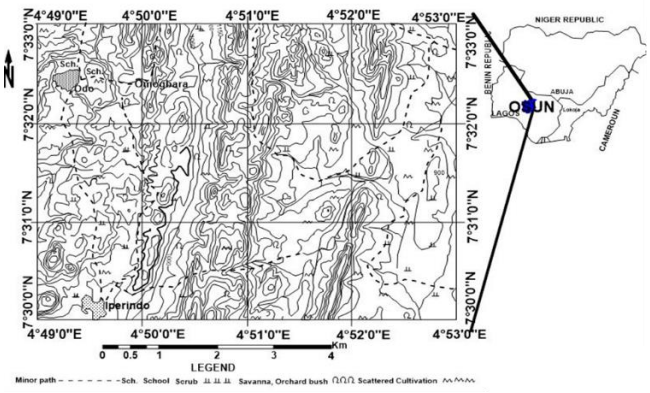

Figure 1: Topographic Map of the Study Area (Insets; Map of Nigeria, after NGSA, 1965).

3.1 Landsat Enhancement

For the purpose of interpretation and clearly identification of the lineaments from LANDSAT ETM+ data, a false color composite band combination of 754 (RGB) was used. This is base on the representative of target on the imagery. The automatic lineament extraction was carried out using Visualizing Image software ENVI™ 4.5 version and Geomatical™ version 10.1. Geomatical™ 10.1 software facilitates the conversion of images into PIX format to become suitable for PCI. Mosaic and subset operations were performed to clip the images for the study area as shown in Figure 2. However, automated lineament extraction techniques had to be used to increase the details of existing data. The main advantages of automated lineament extraction over the manual lineament extraction involves; the ability to uniformly approach the different images, and to perform processing operations in a short module to extract linear features from an image and records the polylines in vector segments by using six parameters. These parameters are obtained from PCI Geomatics™ 10.1 User's Manual.

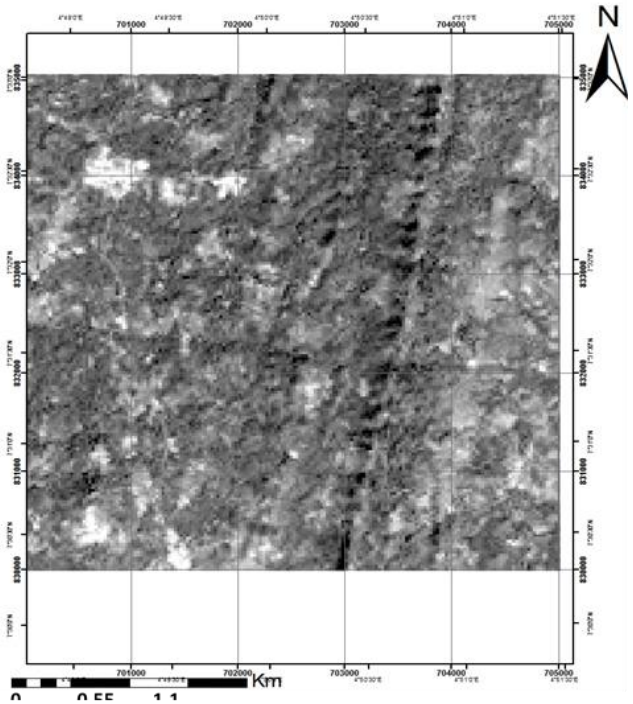

Figure 2: Mosaic Image of the Landsat ETM-7 Satellite Data of the study Area

3.2 Aeromagnetic Enhancement

The aeromagnetic data obtained from Nigerian Geological Survey Agency (NGSA) was gridded into 50m cell size using minimum curvature gridding method to produce total magnetic intensity map. To improve the quality of the data and distinguish the anomalies of interest that are significant to the location of groundwater, the following filters were applied on the total magnetic intensity map (Figure 3). Reduction to equator and derivative filter (horizontal derivative and vertical derivative). The Euler deconvolution of the aeromagnetic field data was done to determine the locations and depths of the source bodies and other geologic sources. Structural index of 2.0 display structural features appropriate for groundwater accumulation. Lineaments were generated by georeferencing and digitizing derivative filter and 3D Euler deconvolution results.

3.3 VLF-EM Survey

Frequency range between 16.6 - 22.2 KHz, readings were taken at the five (5) established traverses (Figure 4) at regular interval of 30metres station separation. The equipment reads the raw real component on the field and the raw imaginary and the filtered were downloaded from the ABEM Wadi VLF equipment after completion of the survey. The profiles of the raw real and the filtered real components were plotted against stations separation. The KHFFILT program (Karous-Hjelt and Fraser filtering of VLF measurements) was used to perform Karous-Hjelt and Fraser filtering on VLF (very-low-frequency) data to generate inverted conductivity sections.

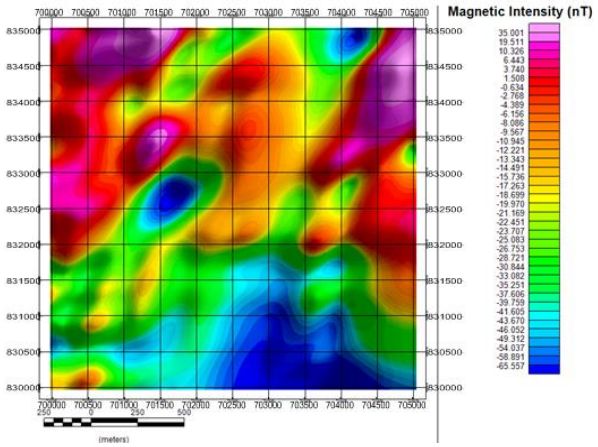

Figure 3: Colour Shaded Aeromagnetic Total Magnetic Intensity (TMI) Map of the Study Area

3.4 Electrical Resistivity Survey

A total of 13 vertical electrical sounding (VES) were carried out in the study area (Figure 4). The results were plotted on a bi-log graph with the apparent resistivity plotted against the electrode spacing AB/2. The curves were partially curve matched using both the master and auxiliary curves for curve matching. Automated inversion of the modeled field data was conducted using Resist software (Vander Velpen, 1988). The parameters displayed at the end of the iterative process are taken to be representative of the geo-electric parameters in terms of thickness and resistivity.

4. Results and Discussion

4.1 Lineament Extraction from Landsat Imagery

Figure 5 shows extracted lineaments from the satellite image. Spatial distributions of groundwater are localized along regional and local fracture patterns that provide conduits along which groundwater flows penetrate host rocks. These fracture patterns has been mapped using the Landsat images (Figure 5). North-eastern and central parts are characterized by very high lineaments while the southern part is observed to have low lineaments density. These lineaments are closely related to tectonic activities resulting in geologic features like fractures, faults and shear zones in the area which is a potential groundwater zone.

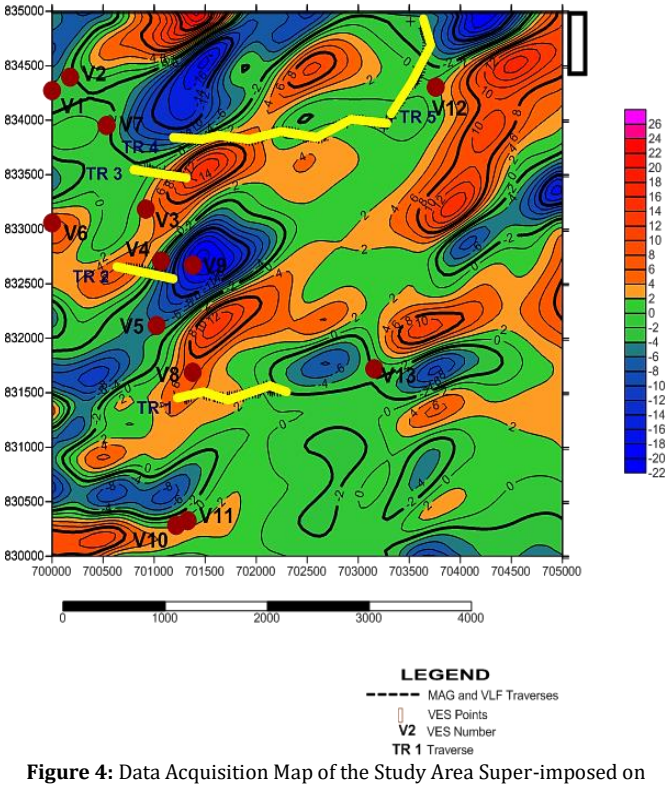

Figure 4: Data Acquisition Map of the Study Area Super-imposed on Residual Map

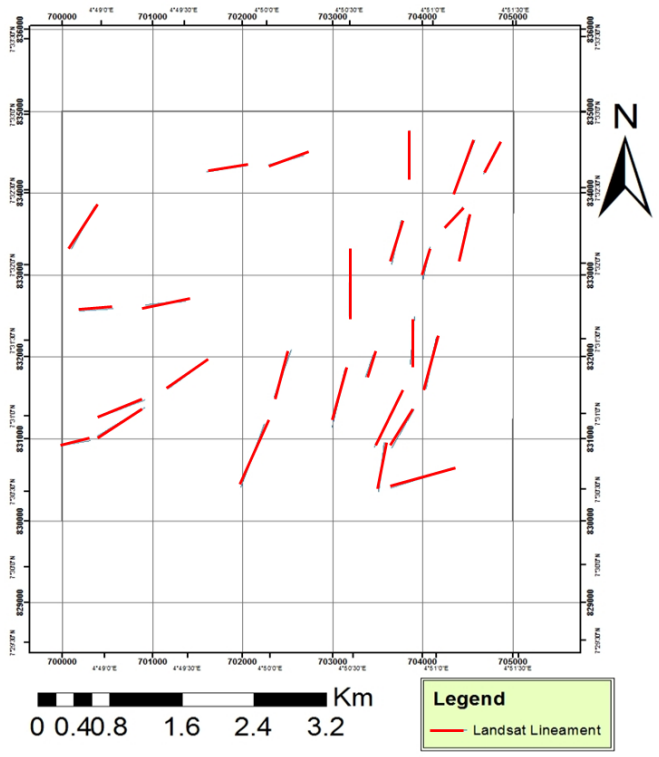

Figure 5: Landsat lineament map of the study area

However, the low lineaments density observed in the northern part of the study area could be due to the thick vegetation cover and deep weathering.

4.2 Aeromagnetic Anomaly Extraction

Figure 6 shows the reduced aeromagnetic data to equator (REDE) map of the magnetic anomalies over the study area. This filtered is normally used to correct for effect of low magnetic latitude and center the peak magnetic anomalies over their corresponding sources.

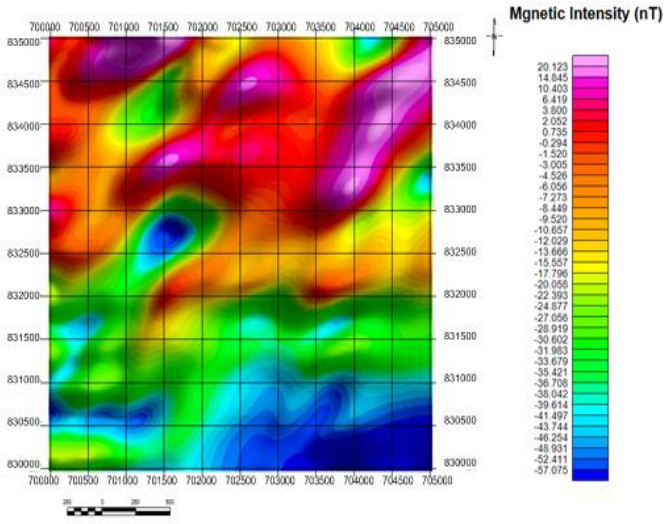

Figure 6: Reduction –to-Equator Map of the Study Area

The southwestern part of the map having relative low magnetic intensity values (-17 nT and -57 nT) marked with green and blue colour suggested geological structures (fracture/fault) hosting the water. Figure 7 shows horizontal derivative Map of the Study Area, which displays detailed information about the structures, contacts and the tectonic setting of the study area. This helped in creating shaded images thereby enhancing the anomalies of smaller and near-surface geological features. From Figure 7, the filter amplifies the NE-SW direction better. The derivative lineament tallied with some lineaments from landsat. On the other hand, vertical derivative (Figure 8) enhances the shallow geologic sources in the data and aided in the definition of the edges of sources bodies. Magnetic anomalies trending NE-SW direction were observed (Figure 8). It should be noted that lineaments from both horizontal and vertical derivatives show good correlation with landsat lineament (Figure5), which are potential location for groundwater.

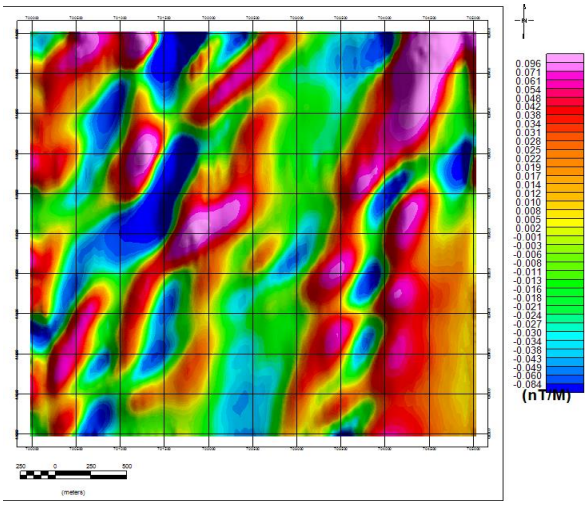

Figure 7: Horizontal derivative Map of the Study Area

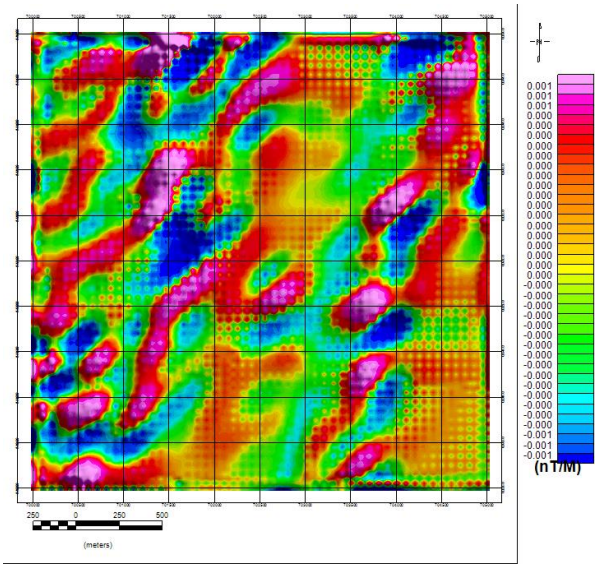

Figure 8: Vertical derivative Map of the Study Area

Figure 9 shows a standard Euler solutions obtained from aeromagnetic data structural index of 2 (SI=2), (i.e. vertical or horizontal cylinder). Figure 9 applies for simple model of a magnetic field caused by the presence of rock contact as potential source for the magnetic anomaly observed in the study area. Depth between 36m and 101m was obtained, which shows relatively shallow depth as related to the delineated rock boundaries. The extracted lineaments reflect the position of features such as faults, deep fractures and geologic contacts.

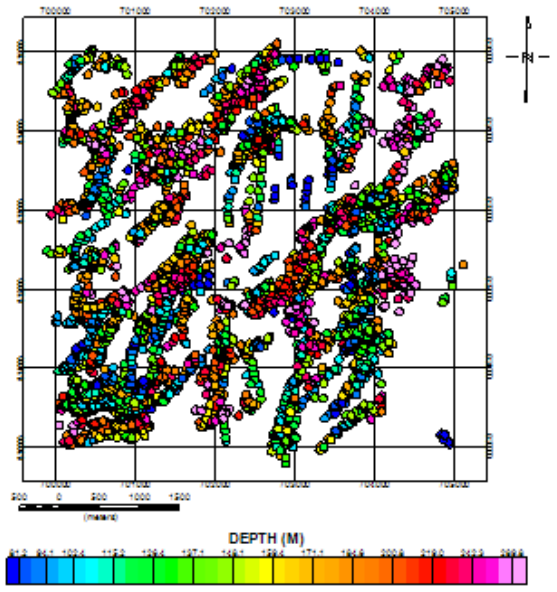

Figure 9: Standard Euler Solutions Obtained from Aeromagnetic Data (SI=2)

The results obtained from derivative maps and 3D Euler solution at Structural Index (S.I=2) were built into ArcGIS environment to generate composite aeromagnetic lineament map of the study area (Figure 10). Most of the magnetic bodies are oriented in the NE-SW and some NW-SE, N-S and W-E directions. These magnetic bodies are principally characteristics of faults and fractures.

Figure 11 shows the lineament intersection map between aeromagnetic and landsat lineaments of the study area. General coincidence of both landsat and aeromagnetic lineaments trends reflect continuous contrasts/fractures at depth.

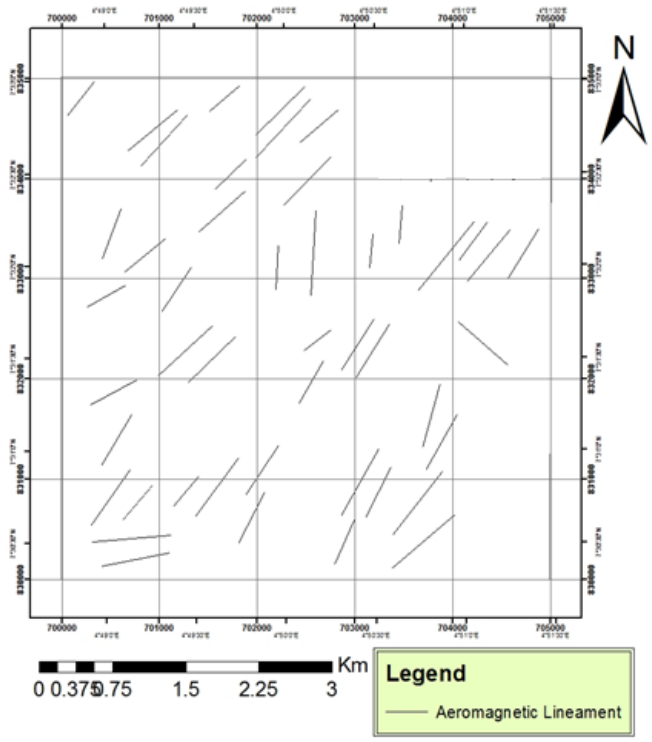

Figure 10: Aeromagnetic lineament Map of the Study Area.

The combined interpretations of aeromagnetic data and Landsat ETM+, added several significant structural elements, that were previously unrecognized from the separated interpretations of aeromagnetic and remotely sensed data. The zones of intersection of these structural trends which are potential sites for groundwater were accordingly delineated at 14 locations. The potential groundwater sites tend to occur in areas with a high density of fractures and a concentration of fracture intersections.

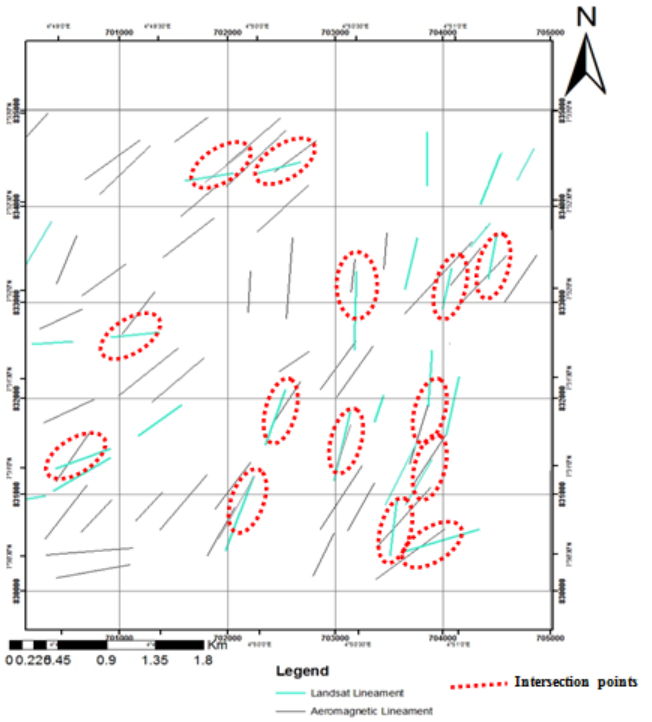

Figure 11: Intersection Lineament Map of the Study Area.

4.3 Electromagnetic Delineation of Potential groundwater Zones

The profile displays and structural evaluation of the VLF-EM data are presented in Figures 12-16. Figure 12a presents the result of the VLF-EM data for traverse 1 and its corresponding 2-D Karous-Hjelt's in current density section. On the 2-D current density section (Figure 12b), the first and second conductive zone were observed at depth up to 125m and 80m. The third conductive zone at distance 660m has a depth of more than 200m and width up to 120m. This third electromagnetic anomaly is an indication of a geologic structure.

On the second traverse (Figure 13), the conductive zones are encountered at distances of 120m, 210m, and 360m. These conductive zones were observed at the depth of 58m, 50m and 45m respectively. The conductive zones are interpreted as pockets of clay from their current density values. Figure 14 shows the VLF profile for traverse 3. It was observed that there was no anomaly from the display of the profile. Electromagnetic anomalies were observed at 360m and 1620m of Figure 15. These anomalies were delineated as pockets of conductive bodies up to about 100m in depth. The conductive anomaly at 840m and 1380m have a depth up to 200m (Figure 14). The anomaly at distance 1140m (Figure 14) has a thickness of about 100m and the depth extends of over 200m, which is likely to be a fault. There is no interpreted electromagnetic anomaly on Figure 16.

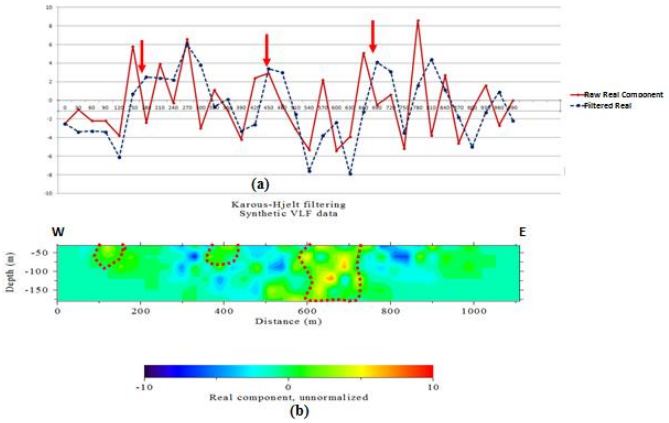

Figure 12: (a) VLF-EM profile for Traverse 1; (b) 2-D Current Density display

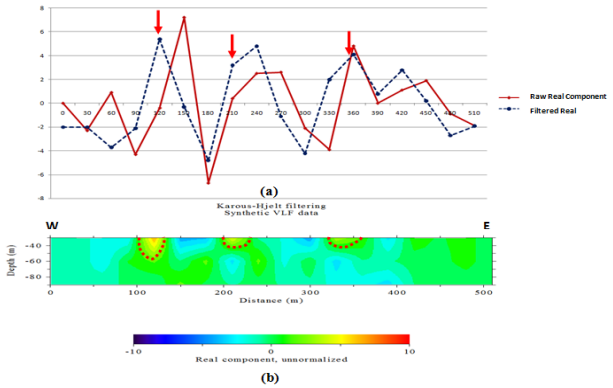

Figure 13: (a) VLF-EM profile for Traverse 2; (b) 2-D Current Density display

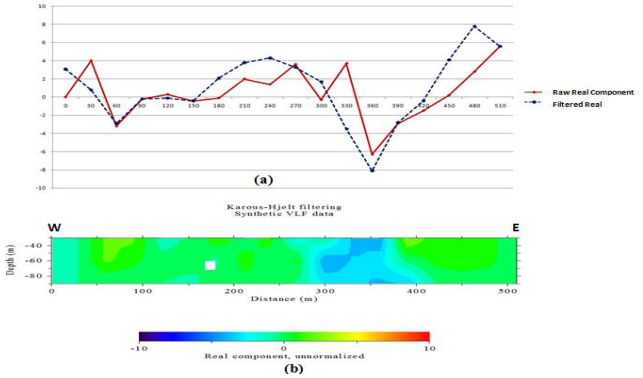

Figure 14: (a) VLF-EM profile for Traverse 3; (b) 2-D Current Density display

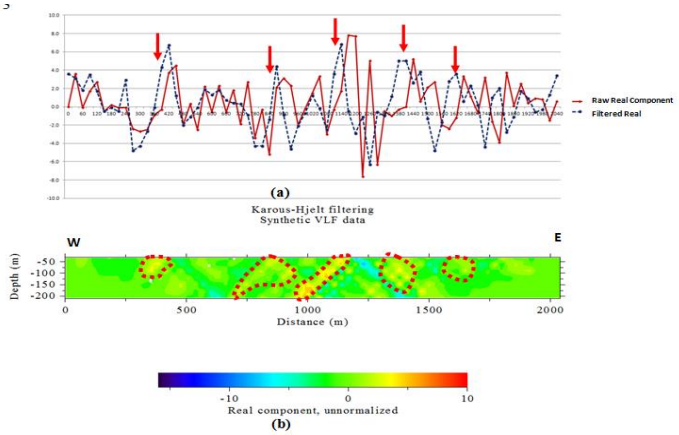

Figure 15: (a) VLF-EM profile for Traverse 4 W-E; (b) 2-D Current Density display

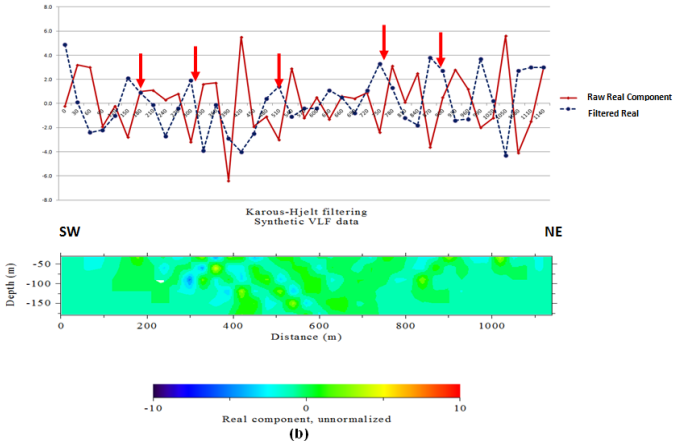

Figure 16: (a) VLF-EM profile for Traverse 5 SW-NE; (b) 2-D Current Density display

4.4 Lithological differentiation from the Vertical Electrical Sounding (VES)

The summaries of identified lithologic units obtained from the characteristic sounding curves are shown in Table 1. The lithologic units vary from 3-5 layers, which includes A, H, K, HK, HA, KH, HKH and KHA. The H, K, HA and KH curve types occupied about 8%. 'A' curve, being the dominant curve type, occupied about 31%, while other curve types occupied the remaining 37%. The A, H and KH curve types are typical of a basement complex environment. The other complex curve types, such as HKH and KHA, are indication of highly fractured areas (Table 1). The geoelectric section in Figure 17 represents the sections along NW-NE part of the field. It revealed four subsurface layers; the topsoil, the weathered layer, the fractured basement and the fresh basement. The weathered layer has a resistivity range of 588 to 817Ωm, with range of thicknesses between 1.4m and 6.7m. at the depth of approximately 2 m. Fractured basement was encountered at the western and eastern part of the profile at depth of approximately 3m and 10 m respectively. These fractured/faulted areas are the point of interest for groundwater.

Figure 18 shows the geoelectric section of VES 6, VES 4 and VES 9 along NW-SE direction, in which four subsurface geologic layers were delineated. These geologic layers are the top soil, the weathered layer, fractured basement and the fresh basement. The weathered layer was encountered at the depth of 1.2 m, with resistivity between 89 and 176Ωm and thicknesses between 2.2m and 6.4m respectively. Fractured basement occur at the western through central part of the section at the depth of 11 m. The geoelectric section of VES 6, VES 3, and VES 12 (Figure 19), approximately along SW-NE direction, revealed a very thin overburden layer (top soil and weathered layer) of 3 m to the fresh basement. The only possible occurrence of groundwater is within the fracture basement, which runs from the west to east of the section at the depth of about 8 m.

4.5 Groundwater potential map of the study area

Figure 20 shows groundwater potential map of the study area, generated from the superposition of the results of landsat, aeromagnetic (maps,

profiles and sections), VLF-EM (profiles and sections) and VES geoelectric parameters complimented with the geological map and the structural map of the study area. Areas with presence of geologic structures and thick overburden layers (top soil and weathered layer) were rated high groundwater potential zones and vice-versa. It was interpreted that the southeastern part, central part and north eastern part of the study area have high groundwater potential while the southwestern part and parts of the central area are classified as low groundwater zones.

Table 1: Summary of Geoelectric Parameters Delineated in the Study Area.

VES No	No of Layers	Resistivity (ohm-m)	Thickness (m)	Depth (m)	Lithology	Curve Type
1	1 2 3	25 149 3726	0.8 6.1 -	0.8 6.9 -	Top soil Weathered Basement Fresh Basement	A
2	1 2 3	210 697 6961	0.6 19.4 -	0.6 20.0 -	Top soil Weathered Basement Fresh Basement	A
3	1 2 3 4	87 500 212 15354	1.5 5.4 10.5 -	1.5 6.9 17.4 -	Top soil Weathered Basement Fractured Basement Fresh Basement	KH
4	1 2 3 4	611 177 1899 208	0.6 2.3 6.6 -	0.6 2.9 9.6 -	Top soil Weathered Basement Fresh Basement Fractured Basement	HK
5	1 2 3	55 97 2784	4.6 7.5 -	4.6 12.1 -	Top soil Weathered Basement Fresh Basement	A
6	1 2 3 4 5	960 609 1609 232 3185	1.5 2.5 7.3 18.1 -	1.5 4.0 11.3 29.4 -	Top soil Weathered Basement Fresh Basement Fractured Basement Fresh Basement	HKH
7	1 2 3 4	117 43 259 9458	10.0 2.5 2.9 -	10.0 12.5 15.4 -	Top soil Weathered Basement Weathered Basement Fresh Basement	HA
8	1 2 3	491 239 822	1.2 6.6 -	1.2 7.9 -	Top soil Weathered Basement Fresh Basement	H
9	1 2 3	23 89 2658	1.0 6.4 -	1.0 7.4 -	Top soil Weathered Basement Fresh Basement	A
10	1 2 3 4	258 767 163 4890	0.7 6.6 13.6 -	0.7 7.3 20.9 -	Top soil Fresh Basement Fractured Basement Fresh Basement	KH
11	1 2 3 4 5	151 588 94 1136 15834	0.8 1.4 4.9 1.5 -	0.8 2.2 7.1 8.6 -	Top soil Weathered Basement Fractured Basement Fresh Basement Fresh Basement	KHA
12	1 2 3 4	258 5720 266 7129	0.8 3.9 6.9 -	0.8 4.7 11.6 -	Top soil Fresh Basement Fractured Basement Fresh Basement	KH
13	1 2 3	837 5534 972	1.1 7.2 -	1.1 8.3 -	Top soil Fresh Basement Fractured Basement	K

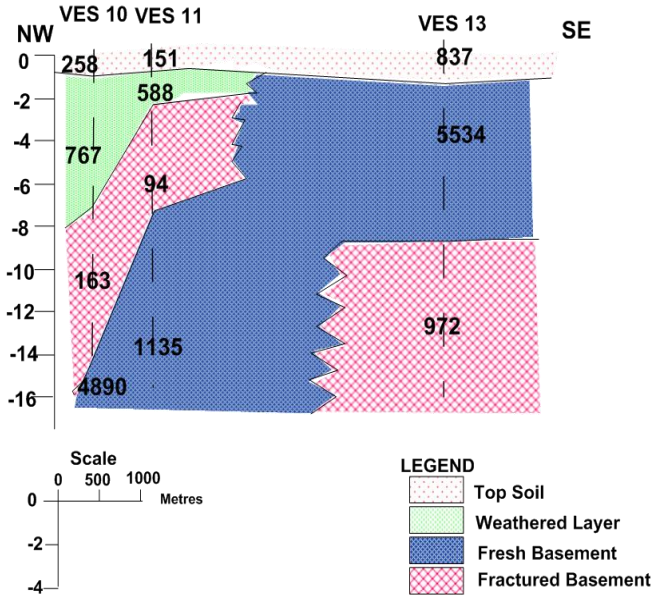

Figure 17: Geoelectric section of VES 10, VES 11 and VES 13 along NW-SE direction in the study area

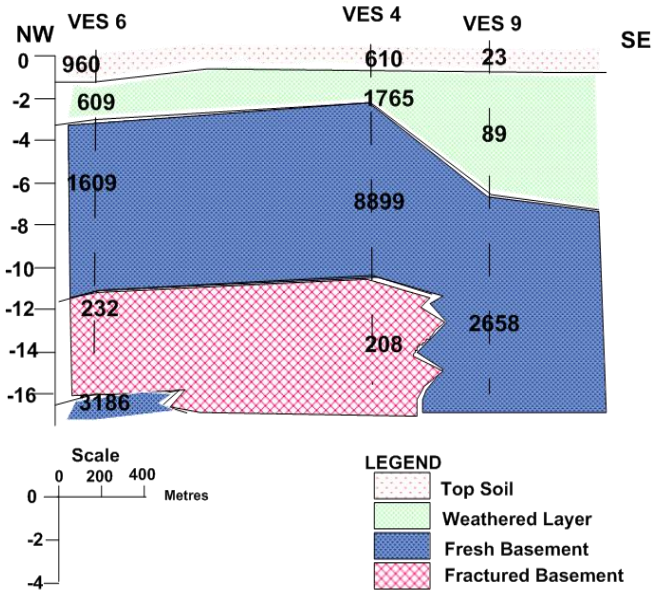

Figure 18: Geoelectric section along VES 6, VES 4 and VES 9 along NW-SE Direction of the study area

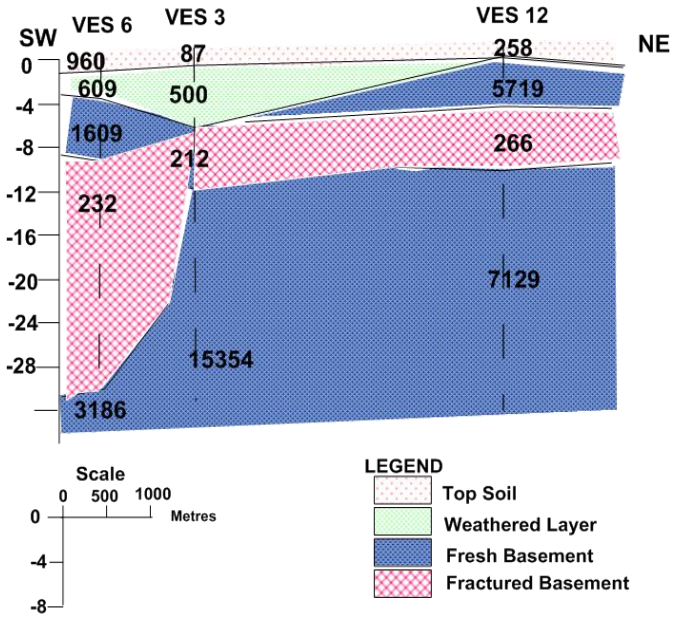

Figure 19: Geoelectric section along VES 6, VES 3 and VES 12 along SW-NE Direction of the study area

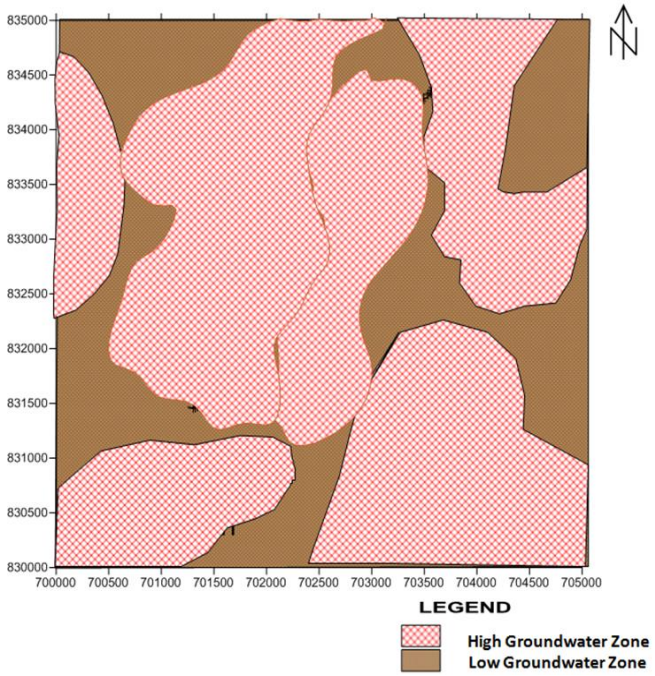

Figure 20: Groundwater potential map of the Study Area

5 Conclusion

In this research, groundwater potential of Iperindo and its environs have been investigated using satellite remotely sensed and other geophysical methods. The study was aimed at delineating the geological feature and its implication on hydrogeologic setting. The investigation involved the extraction of lineaments from Landsat Thematic Mapper (TM) satellite imagery and aeromagnetic. Aeromagnetic data acquired from Geological Survey of Nigeria was interpreted from which total magnetic intensity map was enhanced to improve the quality of the map. Enhancement techniques such as reduction to equator and derivative filter (horizontal and vertical) applied to improve the position of the anomaly features. The aeromagnetic data was used initially to detect and estimate the configuration of basement rocks and locate subsurface faults within the study area which is important for giving a clear overview of the subsurface hydrogeological setting. The 3-D euler deconvolution was also applied to locate and estimate the depth to electromagnetic anomalous bodies, which shows varying depth between 36m and 101m. The lineament of aeromagnetic map was generated from derivative maps and structure index of 2.0. The processed image shows the lineaments trends majorly toward NE-SW directions indicating the direction of the flow of groundwater. General coincidence of both Landsat and aeromagnetic lineaments trends were observed, which means that these lineaments reflect real continuous fault/fractures in depth, as an indicative of potential groundwater aquifer.

The VLF-EM data revealed the existence of linear features, which are interpreted as faults and fractures. These linear features run at approximately NE-SW, W-E, and NW-SE directions. The linear features were observed in the near surface to the depth of up to 60 m. A maximum of four (4) subsurface layers (top soil, weathered layer, fresh basement and fractured basement) were delineated from the qualitative interpretation of the vertical electrical sounding curves. All the results obtained from the integrated geophysical methods indicate high prospect for groundwater development that will be enough for the community planning and distribution for both domestic and commercial uses within the area. However, this study does not address the aquifer vulnerability to pollution created from the mining activities of the area. Therefore, further studies involving the assessment of aquifer vulnerability of the study area, most especially within the high groundwater zones, is encouraged.

References

Ako, B.D., Olorunfemi, M.O., 1989. Geoelectric survey of groundwater in the newer basalts of Vom, Plateau State. Journal of Mining and Geology, 25, Pp. 1-2.

Amadi, U.M.P., and Nurudeen, S.I., 1990. Electromagnetic survey and the search for groundwater in the crystalline basement complex of Nigeria. Journal of Mining Geology, 26, Pp. 45 – 53.

Batista-Rodr´ıguez, Jos´e, A., Caballero, A., P´erez-Flores, M., Carmenates, A., Almaguer, Y., 2017. 3D Inversion of Aeromagnetic Data on Las Tablas District, Panama. Journal of Applied Geophysics. https://doi.org/10.1016/j.jappgeo.2017.01.018

Eaton, G.P., and Watkins, J.S., 1970. The use of seismic refraction and gravity methods in hydrogeological investigations. Proc. Canadian Centennial Conf. Mining and Groundwater Geophysics, Ottawa.

Emujakporue, G., Ofoha, C., Kiani, I., 2017. Investigation into the basement morphology and tectoniclineament using aeromagnetic anomalies of Parts of Sokoto Basin, North Western, Nigeria. Egyptian Journal of Petroleum. https://doi.org/10.1016/j.ejpe.2017.10.003

Federal Government of Nigeria and United Nations children's Fund (UNICEF). 2001. 2002-2007 Master Plan of Operation Country Programme of Co-operation for Nigerian Women and Children. Abuja.

Hung, L.Q., Batelaan, O. De Smedt, F., 2005. Lineament extraction and analysis, comparison of Landsat ETM and Aster imagery. Case study: Suoimuoi tropical karst catchment, Vietnam. Proc. SPIE 5983 (5983), Pp. 1-12.

McNeill, J.D., 1980. Electromagnetic terrain measurement at low induction numbers. Technical note TN. Geonics Limited, Ontario, Canada, Pp. 1-15.

Odeyemi, I.B., 1993. A comparative study of remote sensing images of the structure of okemesi fold belt, Nigeria. ITC J., 1, Pp. 77-81.

Olomo, K.O., 2021. Assessment of groundwater vulnerability based on electrical resistivity-a case study in part of Dahomey Basin, southwestern, Nigeria. Arab J. Geosci., 14 (20), Pp. 2125-2132 https://doi.org/10.1007/s12517-021-08559-1

Olorunfemi, M.O., Dan – Hassan, M.A., and Ojo, A.S., 1995. On the scope and limitations of the electromagnetic methods in groundwater prospecting in a Precambrian basement terrain a Nigerian case study. Journal of Africa Earth Sciences, 20 (2), Pp. 151 – 160.

Olorunfemi, M.O., Fasuyi, S.A., 1993. Aquifer types and the geoelectric/ hydrogeological characteristics of part of the central basement terrain of Nigeria (Niger State). Journal African Earth Science, 16, Pp. 309 – 317.

Osinowo, O., Akanji, A., and Olayinka, A., 2013. Application of high-resolution aeromagnetic data for basement topography mapping of Siluko and environs, southwestern Nigeria. Journal of African Earth Sciences, https://doi.org/10.1016/j.jafrearsci.2013.11.005

Palacky, G.J., Ritsema, I.L., and De Jong, S.J., 1981. Electromagnetic prospecting for Groundwater on the Republic of Upper Volta. Geophysical Prospecting, 29, Pp. 932 – 955.

Satpathy, B.N., and Kanugo, D.N., 1976. Water exploration in hard terrain. A case history. Geophysical Prospecting, 24, Pp. 725 – 736.

Srivastava, A., 2002. Aquifer geometry, basement-topography and ground water quality around Ken Graben,India. *Journal of Spatial Hydrology,* 2(2), Pp. 1-18.

Steinich, B., Bocanegra, G., and Sánchez, E., 1999. Basement topography and fresh-water resources of the coastal aquifer at Acapetahua, Chiapas, Mexico. *Geofísica Internacional,* 38 (2), Pp. 107-115.

Vanderberghe, J., 1982. Geoelectric investigations of a fault system in Quaternary deposits. Geophysical prospecting, 30, Pp. 879 – 897.

Wright, C.P., 1992. The hydrogeology of crystalline basement aquifers in Africa. In: C. P. Wright and W. C. Burgess (eds). Hydrogeology of Crystalline Basement aquifer in Africa. Geological Society of London Special Publication, No. 66, Pp. 1 – 27.